Journal of Nuclear Medicine, published on March 13, 2020 as doi:10.2967/jnumed.119.241414

Prognostic Value of ^{18}F-FDG PET/CT in a Large Cohort of 495 Patients with Advanced Metastatic Neuroendocrine Neoplasms (NEN) Treated with Peptide Receptor Radionuclide Therapy (PRRT)

Jingjing Zhang[1*#], Qingxing Liu[1,2*], Aviral Singh[1,3], Christiane Schuchardt[1], Harshad R. Kulkarni[1], Richard P. Baum[1]

1. THERANOSTICS Center for Molecular Radiotherapy and Precision Oncology, ENETS Center of Excellence, Zentralklinik Bad Berka, Bad Berka, 99437, Germany

2. Department of Nuclear Medicine, Peking Union Medical College Hospital, Chinese Academy of Medical Sciences & Peking Union Medical College, Beijing, 100730, China.

3. GROW-School for Oncology and Developmental Biology, Maastricht University, Netherlands

*Contributed equally to this work

 # For correspondence or reprints contact: Jingjing Zhang, THERANOSTICS Center for Molecular Radiotherapy and Precision Oncology, Zentralklinik Bad Berka, Robert-Koch-Allee 9, 99437 Bad Berka, Germany. Phone: +49 364-585-42216. Fax: +49 364-585-3515. E-mail: zhangjingjingtag@163.com

Running title: Prognostic value of FDG PET/CT in PRRT

Word count: 5894

ABSTRACT

The objective of this retrospective study was to determine the role of ^{18}F-FDG PET/CT in a large cohort of 495 patients with metastatic neuroendocrine neoplasms (NENs) who were treated with peptide receptor radionuclide therapy (PRRT) with a long-term follow-up. **Methods:** The 495 patients were treated with ^{177}Lu- and/or ^{90}Y- DOTATOC/DOTATATE PRRT between 2/2002 and 7/2018. All subjects received both ^{68}Ga-DOTATOC/TATE/NOC and ^{18}F-FDG PET/CT prior to treatment and were followed 3-189 months. Kaplan-Meier analysis, log-rank test (Mantel-Cox), and Cox regression analysis were performed for overall survival (OS) and progression-free survival (PFS). **Results:** 199 patients (40.2%) presented with pancreatic NEN, 49 with CUP (cancer of unknown primary), 139 with midgut NEN, whereas the primary tumor was present in the rectum in 20, in the lung in 38, in the stomach in 8 and other locations in 42 patients. FDG-PET/CT was positive in 382 (77.2%) patients and 113 (22.8%) were FDG-negative before PRRT, while 100% were ^{68}Ga-DOTATOC/TATE/NOC positive. For all patients, the median PFS and OS, defined from start of PRRT, were 19.6 mo and 58.7 mo, respectively. Positive FDG predicted shorter PFS (18.5 mo vs 24.1 mo; p =0.0015) and OS (53.2 mo vs 83.1 mo; p <0.001) than negative FDG. Amongst the pancreatic NEN, the median OS was 52.8 mo in FDG positive and 114.3 mo in FDG negative subjects (p =0.0006). For all patients with positive ^{18}F-FDG uptake, and a ratio of the highest SUVmax on ^{68}Ga-SSTR PET to the most ^{18}F-FDG-avid tumor lesions >2, the median OS was 53.0 mo, compared to 43.4 mo in those patients with a ratio <2 (p =0.030). For patients with

no ^{18}F-FDG uptake (complete “mismatch” imaging pattern), the median OS was 108.3 mo vs 76.9 mo for SUVmax >15.0 and ≤15.0 on ^{68}Ga-SSTR PET/CT, respectively. **Conclusion:** The presence of positive lesions on ^{18}F-FDG PET is an independent prognostic factor in patients with NEN treated with PRRT. Metabolic imaging with ^{18}F-FDG PET/CT compliments the molecular imaging aspect of ^{68}Ga-SSTR PET/CT for the prognosis of survival after PRRT. High SSTR expression combined with negative ^{18}F-FDG PET/CT imaging is associated with the most favorable long-term prognosis.

Key Words: peptide receptor radionuclide therapy; ^{18}F-FDG; neuroendocrine neoplasms; ^{177}Lu; ^{90}Y; prognostic factor

INTRODUCTION

Neuroendocrine neoplasms (NEN) are a heterogeneous group of neoplasms, and typically have a wide range of cellular differentiation with variable biological aggressiveness and clinical outcome(*1*). The clinical course of NEN can be quite heterogeneous with variable response to treatments despite possessing similar tumor characteristics and having received the same therapy. In principle, the choice of therapy depends on individual tumor characteristics and ranges from complete eradication to a "watch and wait" approach(*2-4*). NEN, especially those of the pancreas and intestine, are frequently identified at late stage with advanced metastatic disease.

Most well-differentiated NENs are characterized by a high level of expression of the somatostatin receptors (SSTRs), allowing the use of radiolabeled somatostatin analogs for SSTR targeted imaging (i.e., octreotide scintigraphy or ^{68}Ga-SSTR PET) as well as peptide receptor radionuclide therapy (PRRT), using ^{177}Lu and/or ^{90}Y labeled somatostatin analogs (DOTATATE or DOTATOC). PRRT has been established as an efficient and well-tolerated treatment for patients with unresectable or metastatic progressive well-differentiated SSTR-positive neuroendocrine tumors(*5*), and is shown to be highly efficacious in terms of progression-free survival and response rates compared to other treatment modalities(*6-8*). Quality of life is also significantly improved after PRRT(*7,9,10*). The significant benefit of PRRT over cold somatostatin analog therapy demonstrated by the landmark randomized phase III clinical trial (NETTER-1)(*7*) led to the approval of Lutathera (^{177}Lu-DOTATATE) by both the European Medicines Agency and the U.S. Food and Drug Administration for the treatment of gastroenteropancreatic neuroendocrine tumors.

With the growing importance of PRRT in treating NEN, the relevant outcome predictors are becoming increasingly significant to optimize the application of PRRT. Several prognostic factors of NEN after PRRT have been described including gene cluster expression(*11*), site of the primary tumor(*12,13*), the presence of metastases(*13*), resection of the primary tumor(*14*), grade of differentiation(*13,15-17*), proliferation index (Ki-67 index)(*13,18-20*), serum biomarkers(*18,21*), presence of SSTRs(*22,23*), tumor stage(*24*) and treatment modality(*18,25,26*). However, several of these factors are difficult to assess especially in the setting of multifocal metastatic disease, one such example is the most commonly used proliferation index, Ki-67. Histopathology of a certain small part of the tumor from biopsy or resected specimens may not be representative of the entire tumor burden, and therefore, whole-body noninvasive alternatives may offer significant advantages(*27*).

SSTR imaging (PET or scintigraphy) represents an estimation of the somatostatin receptor status for planning of PRRT as well as evaluation of response to the treatment. ^{18}F-fluorodeoxyglucose (^{18}F-FDG) PET/CT is used to assess glycolytic metabolism, characterized by the potential for malignancy. It seems like a promising alternative to repeated tissue sampling for the determination of the aggressiveness of tumors since it has been found to be associated with tumor aggressiveness and is highly prognostic in a variety of tumors(*28-31*). The diagnostic value of ^{18}F-FDG PET in lower grade (1, II, IIIa) neuroendocrine neoplasms is limited since they represent the slowly proliferating tumors with lower glycolytic activity. ^{18}F-FDG PET (PET/CT or PET/MRI) is not used for diagnosis of NENs and currently not a routine diagnostic for NENs prior to PRRT.

The aim of our study was to evaluate the role of baseline ^{18}F-FDG PET/CT in predicting the progression-free survival (PFS) and overall survival (OS) of a large cohort of patients with metastatic NEN treated with PRRT with a long-term follow-up.

MATERIALS AND METHODS

Patients

From February 2002 to July 2018, a retrospective data analysis was performed for a total of 495 patients with advanced NEN who received PRRT at Zentralklinik Bad Berka (Germany) and underwent PET/CT imaging with both, ^{68}Ga-SSTR and ^{18}F-FDG at baseline prior to therapy. Patients with histopathologically confirmed metastatic NEN and high level of SSTR expression, i.e., tumor uptake greater than or equal to normal liver parenchyma uptake on ^{68}Ga-SSTR PET imaging were included. Disease progression was documented within 3-6 mo prior to start of PRRT. The study was approved by the institutional review board, and written informed consent was obtained from each patient. The baseline demographics of the patients are shown in Table 1.

PRRT Regimen

The DOTA-conjugated somatostatin analogs DOTATOC, DOTANOC, and DOTATATE were labeled with ^{68}Ga for SSTR PET imaging and either ^{177}Lu or ^{90}Y for PRRT, in accordance with good manufacturing practice (GMP) regulations. PRRT regimen were in conformation with the published practical guidelines for PRRT(*32*). The labeling of DOTA-conjugated peptides with ^{177}Lu and ^{90}Y was performed according to a previously published method(*16,33*). High-

performance liquid chromatography was used for quality control. Radiochemical purity was always higher than 98%. An in-house produced amino acid infusion (1600 mL of 5% lysine HCl and 10% L-arginine HCl) was administered for nephroprotection during each PRRT cycle(*34*). Additional nephroprotection using intravenous infusion of 4% Gelofusine (B. Braun Melsungen AG) adjusted to patients' weight (infusion as a bolus of 1 ml/kg body weight over 10 min before therapy and followed by 0.02 ml/kg/min over 3 h after radiopeptide infusion) was applied in cases of impaired renal function (glomerular filtration rate <60 mL/min) as well as in patients treated with ^{90}Y(*16,32*). The infusion was started at least 30 min before administration of the radiopharmaceutical and lasted for 4 h afterwards. The radiopharmaceutical was co-administered over 10-15 min using a second infusion pump system. The administrated radioactivity was individually calculated based on the Bad Berka Score(*8,16,34*).

Response Assessment

The treatment response was evaluated on CT or MR imaging according to RECIST 1.1(*35*) and by molecular imaging (PET) according to European Organization for Research and Treatment of Cancer criteria (EORTC)(*36,37*). Imaging was performed before each PRRT cycle and at restaging. Restaging was performed every 3-4 mo after PRRT, and every 6 mo for stable disease or remission (complete or partial) after initial follow-up, until disease progression. PRRT was resumed if progression occurred after a therapy interval of more than 6 mo (so-called next "treatment phase" of PRRT)(*10,16*). Decision of a salvage approach considering PRRT after progression was taken

by internal or external tumor boards. SSTR PET/CT and ^{18}F-FDG PET/CT (until January 2014 with Siemens Biograph and since then with Biograph mCT Flow 64; Siemens Medical Solutions AG, Erlangen, Germany) was performed in all cases 45-90 minutes after the intravenous injection of 46-260 MBq of ^{68}Ga-DOTANOC, -DOTATOC or DOTATATE, and 45-90 minutes after the intravenous injection of 350-600 MBq of ^{18}F-FDG, respectively. PET/CT images were acquired from the skull to the middle part of the thigh. Contrast-enhanced CT (spiral CT using a Biograph mCT Flow 64) was acquired after the intravenous administration of 60–100 mL of nonionic iodinated contrast agent. Maximum standardized uptake values (SUV_{max}) were obtained by drawing circular regions of interest (ROIs), which were automatically adapted (40% isocontour) to a 3D volume of interest using commercial software provided by the vendor. Images were evaluated by 2 experienced nuclear medicine specialists. MRI was performed in selected cases (allergy to iodinated contrast agent or poor detectability of liver metastases on CT scan), and routine sonography were performed for additional diagnostic evaluation.

Data Analysis

Data was collected in the following categories: patient characteristics, tumor characteristics, prior treatments, baseline ^{68}Ga-SSTR PET/CT, baseline ^{18}F-FDG PET/CT, PRRT radionuclide, PRRT cycle, cumulative activity, all completed ^{68}Ga-SSTR and ^{18}F-FDG PET/CT, and follow-up. Progression was determined based on RECIST and/or EORTC. The categories of tumor uptake and

tumor burden on ^{68}Ga-SSTR and ^{18}F-FDG PET/CT are listed in Table 2 and Supplemental material online.

Statistical Analysis

The primary and secondary endpoints of this study were the duration of OS and PFS, respectively, defined from the start of PRRT. Survival curves for PFS and OS were estimated by Kaplan-Meier analysis, and significance was tested by the log-rank test. Univariate analysis was conducted for each prognostic factor using the log-rank test. Multivariate analysis (Cox proportional-hazard model) was performed to estimate hazard ratios (HR) and 95% confidence intervals (95%CI) for the potential prognostic factors. Quantitative data were denoted as mean ± SD. The statistical analysis was 2-tailed and conducted by SPSS software (IBM). A P value of less than 0.05 was considered statistically significant.

RESULTS

Patient characteristics

The characteristics of 495 patients (299 men, 196 women; median age at first treatment 59.0±10.7 years, range 19-80 years) are shown in Tables 1 and 2. Primary tumors were localized in the pancreas in 199 (40.2%) patients, midgut in 139 (28.1%), lung in 38 (7.7%), rectum in 20 (4.0%), stomach in 8 (1.6%), others in 42 (8.5%) and unknown (cancer of unknown primary, CUP) in 49 patients (9.9%). The majority of patients (117 and 245, respectively) had well differentiated

NENs of grade 1 (23.6%) or grade 2 (49.5%). At baseline, 382 patients (77.2%) were FDG-positive, and 113 (22.8%) were FDG-negative. The number of treatment cycles and cumulative administered radioactivity are listed in Supplemental Table 1. Four hundred and fifteen (83.8%) patients received DUO-PRRT, i.e., a combination of ^{177}Lu and ^{90}Y; 60 (12.1%) received ^{177}Lu as monotherapy and 20 (4.0%) received ^{90}Y as monotherapy. Mean cumulative administered radioactivity for all patients was 25.7±10.8 GBq (range 3.9 GBq-60.7 GBq).

Univariate and Multivariate Analysis for OS and PFS

The results of univariate and multivariate analysis of possible prognostic factors for OS and PFS are listed in Tables 3 and 4. Over a median follow-up for all patients of 94 months (range 3-189 months), 319 patients (64.4%) died and 136 patients (27.5%) progressed by the end of the study. The median OS and PFS of the entire cohort were 58.7 mo (95%CI, 52.8-64.6) and 19.6 mo (95%CI, 17.6-21.7), respectively (Fig. 1).

Tumor grading was an independent predictor for both OS (P=0.012) and PFS (P=0.039). A higher tumor grade was associated with worse prognosis. The median OS in G1, G2 and G3 was 78.5 mo (95%CI, 66.2-90.8), 55.4 mo (95%CI, 46.9-63.9), and 33.2 mo (95%CI, 18.8-47.6), respectively. When compared with G1, G2 had a 1.4-fold increase in the risk of death (95%CI, 1.0-2.0; P, 0.038), while G3 was associated with a 2.5-fold increase (95%CI, 1.3-4.5; P, 0.004). The median PFS in G1, G2 and G3 was 23.0 mo (95%CI, 15.9-30.2), 18.9 mo (95%CI, 15.2-22.6), 7.5 mo (95%CI, 0.0-20.1), respectively. When compared with G1, G2 tumors had a 1.2-fold increase

in the risk of progression (95%CI, 0.9-1.5; P, 0.150), while G3 was associated with a 2.1-fold increased risk of progression (95%CI, 1.3-3.4; P, 0.003).

Primary tumor site was an independent predictor of OS (P=0.004). The median OS of patients with pancreas, midgut and lung NENs were 54.4 mo (95%CI, 49.3-59.6), 77.8 mo (95%CI, 61.0-94.6), and 46.2 mo (95%CI, 34.1-58.3), respectively. The median PFS was 25.8 mo (95% CI, 21.8-29.8), 22.6 mo (95%CI, 17.2-28.0), and 10.6 mo (95%CI, 5.0-16.1), respectively.

^{18}F-FDG Uptake Status Related to Survival

In all patients, median OS and PFS were significantly higher in the ^{18}F-FDG-negative group compared to the ^{18}F-FDG-positive group. The benefit in OS was 83.1 mo (95%CI, 57.0-109.2) versus 53.2 mo (95%CI, 49.4-57.0), P<0.001, respectively, and in PFS, 24.1 (95%CI, 19.9-28.3) versus 18.5 mo (95%CI, 15.9-21.1), P<0.002, respectively (Fig. 2). ^{18}F-FDG-negative status was an independent prognostic factor for OS, with a 0.5-fold decrease in the risk of death (HR, 0.5; 95%CI, 0.3–0.8; P, 0.002) as well as for PFS, with a 0.7-fold decrease in the risk of progression (HR, 0.7; 95%CI, 0.5–0.9; P, 0.007). FDG-positive lymph node and liver tumor burden on ^{18}F-FDG PET imaging were independent predictors for OS (P=0.035 and P=0.034, respectively), whereas, FDG-avid bone tumor burden (metastases) was an independent predictor for PFS (P=0.001).

In the ^{177}Lu-PRRT subgroup, median OS and PFS were significantly higher in the ^{18}F-FDG-negative than in the ^{18}F-FDG-positive group (median OS: 97.7 mo vs 51.0 mo P<0.01) and median PFS: 33.8 mo vs 19.9 mo, P<0.05) (Fig. 3).

In the pancreatic NEN subgroup, median OS and PFS were significantly higher in the ^{18}F-FDG-negative than in the ^{18}F-FDG-positive group (median OS: 114.3 mo vs 52.8 mo and median PFS: 36.9 mo vs 22.4 mo, respectively; for both P<0.001) (Fig. 4).

In the midgut NEN subgroup, the median OS was 95.3 mo in the ^{18}F-FDG-negative group and 62.1 mo in the ^{18}F-FDG PET-positive group. The median PFS was 36.1 mo in the ^{18}F-FDG-negative group and 29.0 mo in the ^{18}F-FDG PET-positive group.

^{68}Ga-SSTR PET Imaging Related to Survival

^{68}Ga-SSTR uptake of primary tumor was an independent predictor of OS (P=0.011) and PFS (P=0.003). In multivariate analysis, compared to Level 1 (L1) liver tumor burden in ^{68}Ga-SSTR PET, L2 had a significant decreased risk of progression with a HR of 0.5 (95%CI, 0.3-0.7; P=0.001), but L3 and L4 had no significant decrease in risk (L3, HR: 0.9, 95%CI: 0.5-1.5, P=0.664; L4, HR: 0.9, 95%CI: 0.6-1.1, P=0.256).

The statistical analysis revealed that the highest SUV_{max} of all target (SSTR-positive) lesions on ^{68}Ga-SSTR PET of each patient was not significant in terms of OS and PFS, and there was no direct correlation between OS and the highest SUV_{max} of all target tumor lesions (P>0.05). The analysis of OS showed no significant difference between patients with SUV_{max}<15 and SUV_{max}>15 on ^{68}Ga-

SSTR PET imaging, including those from the midgut NEN subgroup and the ^{18}F-FDG-negative group. For ^{18}F-FDG-positive patients, with a ratio of maximum SSTR/FDG, which was defined as the highest SUVmax amongst all target lesions on ^{68}Ga-SSTR PET to the most ^{18}F-FDG-avid tumor lesions for each patient >2, the median OS was 53.0 mo, compared to 43.4 mo in patients with a ratio of <2 (P=0.030). For ^{18}F-FDG-negative patients, the median OS was 108.3 mo vs 76.9 mo for a SUV_{max} >15.0 and an SUV_{max} ≤15.0 on ^{68}Ga-SSTR PET, respectively.

DISCUSSION

To the best of our knowledge, to date this represents the largest cohort of metastatic NENs patients treated with personalized PRRT in which long-term prognosis was evaluated on the basis of initial dual PET tracer imaging (^{68}Ga-SSTR PET/CT and ^{18}F-FDG PET/CT). All patients were followed up until death (64.4 percent of the patients) or the study cutoff date (end of 2018). The follow-up (median, 94 mo; range 3-189 mo) in this patient cohort is the longest among all published relevant studies(*16*).

SSTR PET/CT imaging with ^{68}Ga-labelled somatostatin analogs has excellent sensitivity and specificity for diagnosing and staging NEN(*38,39*). ^{18}F-FDG PET is widely used in oncology, but its use in neuroendocrine tumors has been a matter of controversy(*40*). Several studies have demonstrated the association of ^{18}F-FDG PET with treatment response and PFS after PRRT in NENs. In a study with 98 NEN patients, ^{18}F-FDG SUV_{max}>3 was found to be the only independent predictor of PFS and ^{18}F-FDG SUV_{max}>9 was strongly correlated with a greater risk of mortality

although its median OS was not reached(*27*). Sansovini et al. reported a phase II trial of ^{177}Lu-DOTATATE PRRT in 60 patients with locally advanced or metastatic well-differentiated G1/G2 pancreatic neuroendocrine tumors, who completed the scheduled 5 cycles of PRRT. The median PFS was 21.1 mo in FDG-positive patients (58%) and 68.7 mo in the FDG-negative group regardless of the total activity administered ($p<0.0002$)(*41*), but the uptake on somatostatin receptor imaging, pre-therapy and post-therapy, was not significant in terms of PFS(*42*). Chan et al. reported a NETPET grading scheme for dual SSTR/FDG PET/CT imaging in a study with 62 NEN patients. The NETPET grade divided subjects into solely SSTR-positive, SSTR-positive/FDG-positive disease, and SSTR-negative/FDG-positive subgroups and introduced a 0-5 categorical scale largely based on the characteristics of the single initial lesion, showing promise as a prognostic imaging biomarker in neuroendocrine tumors(*43*). Our group also has demonstrated that PET/CT imaging with ^{18}F-FDG along with SSTR helps to stratify patients with WHO G3 NENs(*16*).

The median OS of the current study after PRRT was 58.7 mo within the reported range in literature(*18*). The median PFS was 19.6 mo, which was shorter in comparison to other studies, as the treatment response was evaluated according to both RECIST and molecular imaging criteria. Moreover, the current study included 128 patients who received up to 3 cycle of PRRT only, which may have influenced the prognosis. Meanwhile, this study included not only G1/G2 NEN, but also high-risk G3 NEN, as well as patients with variable primary tumor sites. In this study, both tumor grading and primary tumor site were demonstrated as an independent predictor for OS. Patients

with midgut NEN had the longest median OS of 77.8 mo; whereas, it was 55.4 mo in the rectal NEN group, 54.4 in pancreatic NEN, and 46.2 mo in lung NEN.

Our results demonstrated that ^{18}F-FDG-negative tumor status was an independent prognostic factor for OS of PRRT, with a 0.5-fold decrease in the risk of death. Although not generally used for the diagnosis of NEN, ^{18}F-FDG PET/CT was able to classify NEN patients into different prognostic categories for PRRT. A very high SUV on FDG PET would at least lead to reconsider the decision to perform PRRT as the first line procedure. We would suggest the decision to perform FDG PET/CT on personalized medicine criteria, especially the grading, time course of the disease, speed of progression, total tumor mass, and other criteria as the published Bad Berka Score(*8,16,34*).

SSTR imaging is a positive prognostic factor for demonstrating the abundance of SSTR expression, which is intensively related to well-differentiated tumor, and therefore utilized for evaluating the possibility of treatment with cold and radiolabeled somatostatin analogs(*44*). In this study, ^{68}Ga-SSTR uptake of primary tumor was an independent predictor of OS and PFS, which is in agreement with other studies. However, the prognostic value of ^{68}Ga-SSTR PET imaging was found to be lower than that of the ^{18}F-FDG PET. There was no direct correlation between the single highest SUV_{max} of ^{68}Ga-SSTR PET and OS. For all patients with positive ^{18}F-FDG uptake (NETPET $SSTR^{+}/FDG^{+}$ disease), and a ratio of the highest SUV_{max} on ^{68}Ga-SSTR PET to the most ^{18}F-FDG-avid tumor lesions >2, the median OS was higher than those patients with a ratio <2 ($p=0.030$).

One of the limitations of this study is that it is a retrospective analysis (however, with prospective data sampling using a structured database). There were variations in radioisotopes and SSTR affinities because different radiopharmaceuticals were used. Another limitation is the lack of availability of the exact Ki-67 index in 104 (21%) patients; however, these patients were referred from other centers with histopathologically confirmed NEN without reporting the Ki-67 index, and relevant tissue specimens were not available for re-evaluation. Furthermore, concerning the value of somatostatin receptor uptake for predicting survival receiving PRRT, this study only analyzed the single highest SUV_{max} amongst all target lesions on ^{68}Ga-SSTR PET for each patient. The metastatic tumor burden score on ^{68}Ga-SSTR PET, further genomic signature and the association between survival and comprehensive individual evaluation of somatostatin receptor expression remain warranted.

CONCLUSION

^{18}F-FDG PET/CT demonstrating glycolytic activity, or lack thereof, is an independent prognostic factor in patients with NEN treated with PRRT. FDG-negative NEN demonstrated better OS and PFS compared to FDG-positive NEN, particularly in pancreatic NEN. High uptake on ^{68}Ga-SSTR PET/CT combined with negative ^{18}F-FDG PET/CT is associated with a comparatively prolonged progression free as well overall survival.

DISCLOSURE

No potential conflict of interest relevant to this article was reported.

ACKNOWLEDGMENT

We thank the patients who participated in this study and all research support staff, the radiopharmacists, radiochemists, physician colleagues, nursing staff, and nuclear medicine technologists, past and present, at Zentralklinik Bad Berka for their support.

KEY POINTS

QUESTION: Is ^{18}F-FDG PET an independent prognostic factor in patients with neuroendocrine neoplasms treated with peptide receptor radionuclide therapy (PRRT) and useful in NEN patients following PRRT?

PERTINENT FINDINGS: This large cohort study revealed the presence of positive lesions on ^{18}F-FDG PET is an independent prognostic factor in patients with NEN treated with PRRT. A significant difference was found in both, progression-free survival (PFS) and overall survival (OS) between FDG-positive and FDG-negative patients, respectively.

IMPLICATIONS FOR PATIENT CARE: Metabolic imaging with ^{18}F-FDG PET/CT compliments the molecular imaging aspect of ^{68}Ga-SSTR PET/CT for the prognosis of survival of NEN patients after PRRT.

REFERENCES

1. Huguet I, Grossman AB, O'Toole D. Changes in the Epidemiology of Neuroendocrine Tumours. *Neuroendocrinology.* 2017;104:105-111.

2. Modlin IM, Oberg K, Chung DC, et al. Gastroenteropancreatic neuroendocrine tumours. *Lancet Oncol.* 2008;9:61-72.

3. Falconi M, Eriksson B, Kaltsas G, et al. ENETS Consensus Guidelines Update for the Management of Patients with Functional Pancreatic Neuroendocrine Tumors and Non-Functional Pancreatic Neuroendocrine Tumors. *Neuroendocrinology.* 2016;103:153-171.

4. Fazio N. Watch and wait policy in advanced neuroendocrine tumors: What does it mean? *World J Clin Oncol.* 2017;8:96-99.

5. Bodei L, Herrmann K, Baum RP, Kidd M, Malczewska A, Modlin IM. Caveat Emptor: Let Our Acclaim of the Apotheosis of PRRT Not Blind Us to the Error of Prometheus. *J Nucl Med.* 2019;60:7-8.

6. Werner RA, Weich A, Kircher M, et al. The theranostic promise for Neuroendocrine Tumors in the late 2010s - Where do we stand, where do we go? *Theranostics.* 2018;8:6088-6100.

7. Strosberg J, El-Haddad G, Wolin E, et al. Phase 3 Trial of (177)Lu-Dotatate for Midgut Neuroendocrine Tumors. *N Engl J Med.* 2017;376:125-135.

8. Baum RP, Kulkarni HR, Carreras C. Peptides and receptors in image-guided therapy: theranostics for neuroendocrine neoplasms. *Semin Nucl Med.* 2012;42:190-207.

9. Strosberg J, Wolin E, Chasen B, et al. Health-Related Quality of Life in Patients With Progressive Midgut Neuroendocrine Tumors Treated With (177)Lu-Dotatate in the Phase III NETTER-1 Trial. *J Clin Oncol.* 2018;36:2578-2584.

10. Baum RP, Kulkarni HR, Singh A, et al. Results and adverse events of personalized peptide receptor radionuclide therapy with (90)Yttrium and (177)Lutetium in 1048 patients with neuroendocrine neoplasms. *Oncotarget.* 2018;9:16932-16950.

11. Bodei L, Kidd M, Modlin IM, et al. Measurement of circulating transcripts and gene cluster analysis predicts and defines therapeutic efficacy of peptide receptor radionuclide therapy (PRRT) in neuroendocrine tumors. *Eur J Nucl Med Mol Imaging.* 2016;43:839-851.

12. Kong G, Thompson M, Collins M, et al. Assessment of predictors of response and long-term survival of patients with neuroendocrine tumour treated with peptide receptor chemoradionuclide therapy (PRCRT). *Eur J Nucl Med Mol Imaging.* 2014;41:1831-1844.

13. Panzuto F, Nasoni S, Falconi M, et al. Prognostic factors and survival in endocrine tumor patients: comparison between gastrointestinal and pancreatic localization. *Endocr Relat Cancer.* 2005;12:1083-1092.

14. Bertani E, Fazio N, Radice D, et al. Resection of the Primary Tumor Followed by Peptide Receptor Radionuclide Therapy as Upfront Strategy for the Treatment of G1-G2 Pancreatic Neuroendocrine Tumors with Unresectable Liver Metastases. *Ann Surg Oncol.* 2016;23:981-989.

15. Lee ST, Kulkarni HR, Singh A, Baum RP. Theranostics of Neuroendocrine Tumors. *Visc Med.* 2017;33:358-366.

16. Zhang J, Kulkarni HR, Singh A, Niepsch K, Muller D, Baum RP. Peptide Receptor Radionuclide Therapy in Grade 3 Neuroendocrine Neoplasms: Safety and Survival Analysis in 69 Patients. *J Nucl Med.* 2019;60:377-385.

17. Carlsen EA, Fazio N, Granberg D, et al. Peptide receptor radionuclide therapy in gastroenteropancreatic NEN G3: a multicenter cohort study. *Endocr Relat Cancer.* 2019;26:227-239.

18. Aalbersberg EA, Huizing DM, Walraven I, et al. Parameters to predict progression free and overall survival after peptide receptor radionuclide therapy: a multivariate analysis in 782 patients. *J Nucl Med.* 2019.

19. Nicolini S, Severi S, Ianniello A, et al. Investigation of receptor radionuclide therapy with (177)Lu-DOTATATE in patients with GEP-NEN and a high Ki-67 proliferation index. *Eur J Nucl Med Mol Imaging.* 2018;45:923-930.

20. Thang SP, Lung MS, Kong G, et al. Peptide receptor radionuclide therapy (PRRT) in European Neuroendocrine Tumour Society (ENETS) grade 3 (G3) neuroendocrine neoplasia (NEN) - a single-institution retrospective analysis. *Eur J Nucl Med Mol Imaging.* 2018;45:262-277.

21. Seregni E, Ferrari L, Bajetta E, Martinetti A, Bombardieri E. Clinical significance of blood chromogranin A measurement in neuroendocrine tumours. *Ann Oncol.* 2001;12 Suppl 2:S69-72.

22. Panagiotidis E, Alshammari A, Michopoulou S, et al. Comparison of the Impact of 68Ga-DOTATATE and 18F-FDG PET/CT on Clinical Management in Patients with Neuroendocrine Tumors. *J Nucl Med.* 2017;58:91-96.

23. Haug AR, Auernhammer CJ, Wangler B, et al. 68Ga-DOTATATE PET/CT for the early prediction of response to somatostatin receptor-mediated radionuclide therapy in patients with well-differentiated neuroendocrine tumors. *J Nucl Med.* 2010;51:1349-1356.

24. Rindi G, Kloppel G, Couvelard A, et al. TNM staging of midgut and hindgut (neuro) endocrine tumors: a consensus proposal including a grading system. *Virchows Arch.* 2007;451:757-762.

25. Hellman P, Lundstrom T, Ohrvall U, et al. Effect of surgery on the outcome of midgut carcinoid disease with lymph node and liver metastases. *World J Surg.* 2002;26:991-997.

26. Naraev BG, Ramirez RA, Kendi AT, Halfdanarson TR. Peptide Receptor Radionuclide Therapy for Patients With Advanced Lung Carcinoids. *Clin Lung Cancer.* 2019.

27. Binderup T, Knigge U, Loft A, Federspiel B, Kjaer A. 18F-fluorodeoxyglucose positron emission tomography predicts survival of patients with neuroendocrine tumors. *Clin Cancer Res.* 2010;16:978-985.

28. Kwee TC, Basu S, Saboury B, Ambrosini V, Torigian DA, Alavi A. A new dimension of FDG-PET interpretation: assessment of tumor biology. *Eur J Nucl Med Mol Imaging.* 2011;38:1158-1170.

29. Van den Wyngaert T, Helsen N, Carp L, et al. Fluorodeoxyglucose-Positron Emission Tomography/Computed Tomography After Concurrent Chemoradiotherapy in Locally Advanced Head-and-Neck Squamous Cell Cancer: The ECLYPS Study. *J Clin Oncol.* 2017;35:3458-3464.

30. Meignan M, Cottereau AS, Versari A, et al. Baseline Metabolic Tumor Volume Predicts Outcome in High-Tumor-Burden Follicular Lymphoma: A Pooled Analysis of Three Multicenter Studies. *J Clin Oncol.* 2016;34:3618-3626.

31. Hutchings M, Kostakoglu L, Zaucha JM, et al. In vivo treatment sensitivity testing with positron emission tomography/computed tomography after one cycle of chemotherapy for Hodgkin lymphoma. *J Clin Oncol.* 2014;32:2705-2711.

32. Bodei L, Mueller-Brand J, Baum RP, et al. The joint IAEA, EANM, and SNMMI practical guidance on peptide receptor radionuclide therapy (PRRNT) in neuroendocrine tumours. *Eur J Nucl Med Mol Imaging.* 2013;40:800-816.

33. Wehrmann C, Senftleben S, Zachert C, Muller D, Baum RP. Results of individual patient dosimetry in peptide receptor radionuclide therapy with 177Lu DOTA-TATE and 177Lu DOTA-NOC. *Cancer Biother Radiopharm.* 2007;22:406-416.

34. Baum RP, Kulkarni HR. THERANOSTICS: From Molecular Imaging Using Ga-68 Labeled Tracers and PET/CT to Personalized Radionuclide Therapy - The Bad Berka Experience. *Theranostics.* 2012;2:437-447.

35. Eisenhauer EA, Therasse P, Bogaerts J, et al. New response evaluation criteria in solid tumours: revised RECIST guideline (version 1.1). *Eur J Cancer.* 2009;45:228-247.

36. Young H, Baum R, Cremerius U, et al. Measurement of clinical and subclinical tumour response using [18F]-fluorodeoxyglucose and positron emission tomography: review and 1999

EORTC recommendations. European Organization for Research and Treatment of Cancer (EORTC) PET Study Group. *Eur J Cancer.* 1999;35:1773-1782.

37. Khan S, Krenning EP, van Essen M, Kam BL, Teunissen JJ, Kwekkeboom DJ. Quality of life in 265 patients with gastroenteropancreatic or bronchial neuroendocrine tumors treated with [177Lu-DOTA0,Tyr3]octreotate. *J Nucl Med.* 2011;52:1361-1368.

38. Deppen SA, Liu E, Blume JD, et al. Safety and Efficacy of 68Ga-DOTATATE PET/CT for Diagnosis, Staging, and Treatment Management of Neuroendocrine Tumors. *J Nucl Med.* 2016;57:708-714.

39. Gabriel M, Decristoforo C, Kendler D, et al. 68Ga-DOTA-Tyr3-octreotide PET in neuroendocrine tumors: comparison with somatostatin receptor scintigraphy and CT. *J Nucl Med.* 2007;48:508-518.

40. Nilica B, Waitz D, Stevanovic V, et al. Direct comparison of (68)Ga-DOTA-TOC and (18)F-FDG PET/CT in the follow-up of patients with neuroendocrine tumour treated with the first full peptide receptor radionuclide therapy cycle. *Eur J Nucl Med Mol Imaging.* 2016;43:1585-1592.

41. Sansovini M, Severi S, Ianniello A, et al. Long-term follow-up and role of FDG PET in advanced pancreatic neuroendocrine patients treated with (177)Lu-D OTATATE. *Eur J Nucl Med Mol Imaging.* 2017;44:490-499.

42. Paganelli G, Sansovini M, Scarpi E. Reply to: Predicting the outcome of peptide receptor radionuclide therapy in neuroendocrine tumors: the importance of dual-tracer imaging. *Eur J Nucl Med Mol Imaging.* 2017;44:1777-1778.

43. Chan DL, Pavlakis N, Schembri GP, et al. Dual Somatostatin Receptor/FDG PET/CT Imaging in Metastatic Neuroendocrine Tumours: Proposal for a Novel Grading Scheme with Prognostic Significance. *Theranostics.* 2017;7:1149-1158.

44. Miederer M, Seidl S, Buck A, et al. Correlation of immunohistopathological expression of somatostatin receptor 2 with standardised uptake values in 68Ga-DOTATOC PET/CT. *Eur J Nucl Med Mol Imaging.* 2009;36:48-52.

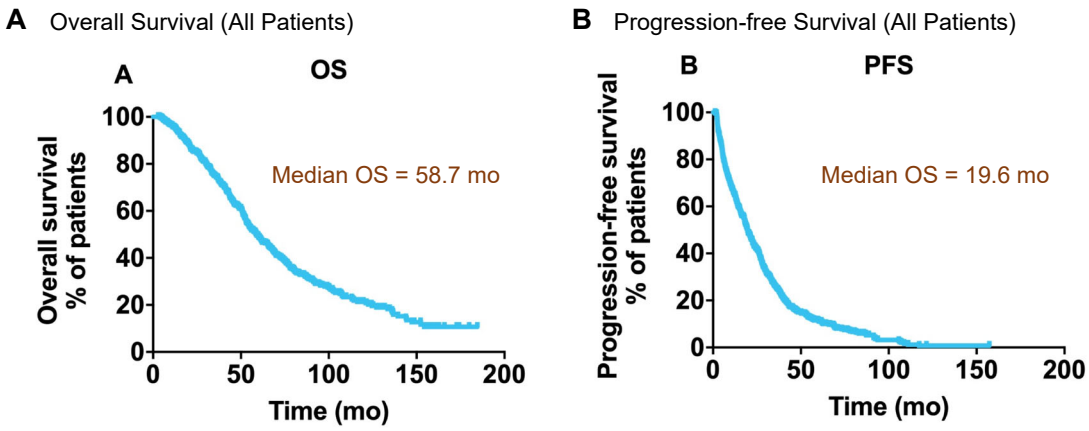

Fig 1. Kaplan-Meier curves of OS and PFS for all patients (n = 495). **(A)** The median OS was 58.7 mo (95% CI, 52.8-64.6). **(B)** The median PFS was 19.6 mo (95% CI, 17.6-21.7).

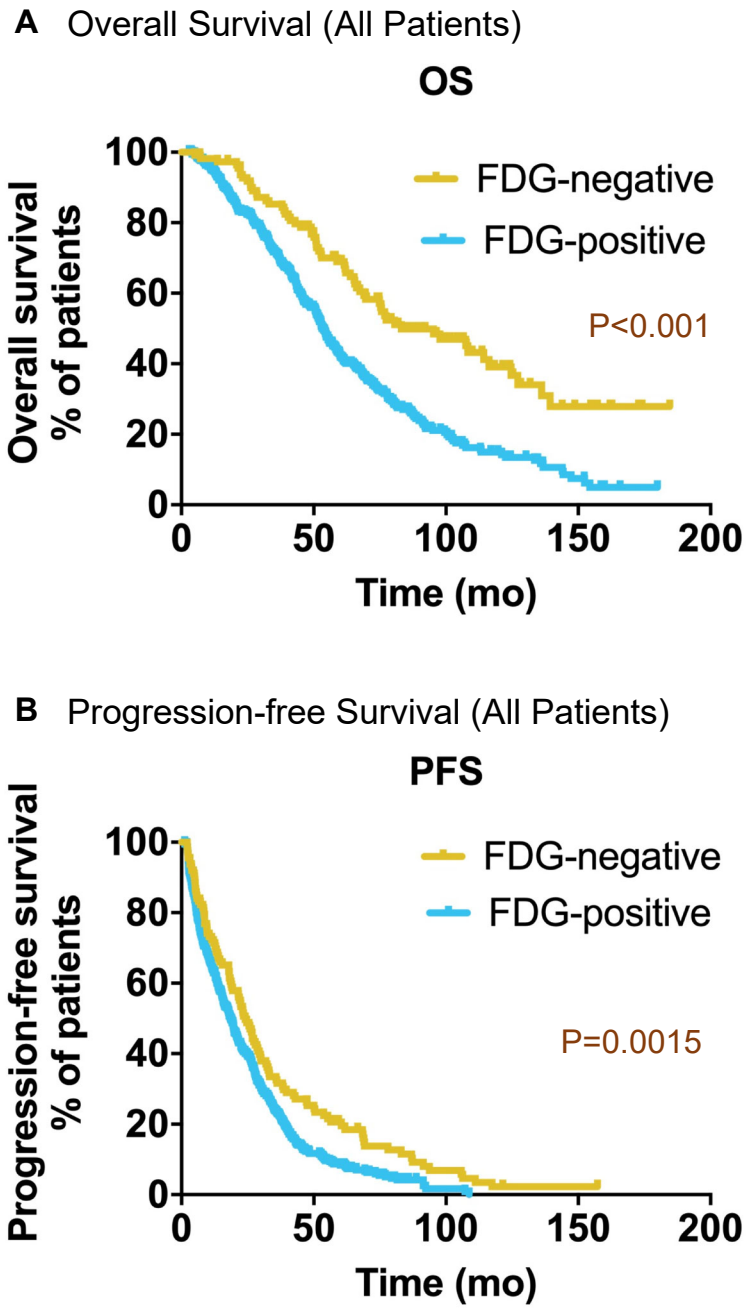

Fig 2. Kaplan-Meier survival analysis of all NEN patients (n=495) stratified by baseline ^{18}F-FDG status. Patients with FDG-negative lesions had significantly higher median OS (A, median OS, 83.1 mo vs 53.2 mo, P<0.001) and higher median PFS (B, 24.1 mo versus 18.5 mo, P<0.002) than patients with FDG-positive lesions.

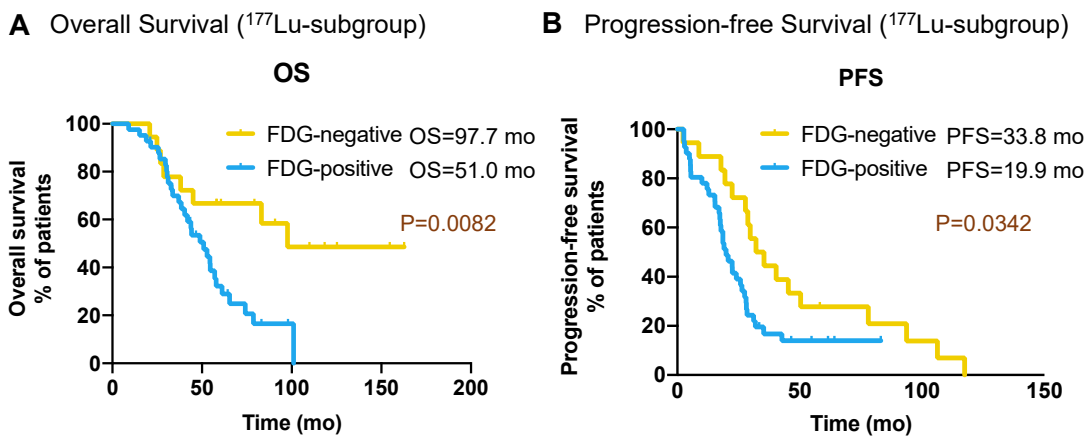

Fig 3. Kaplan-Meier curves of OS (A) and PFS (B) for ^{177}Lu-subgroup (n=60) stratified by baseline ^{18}F-FDG status.

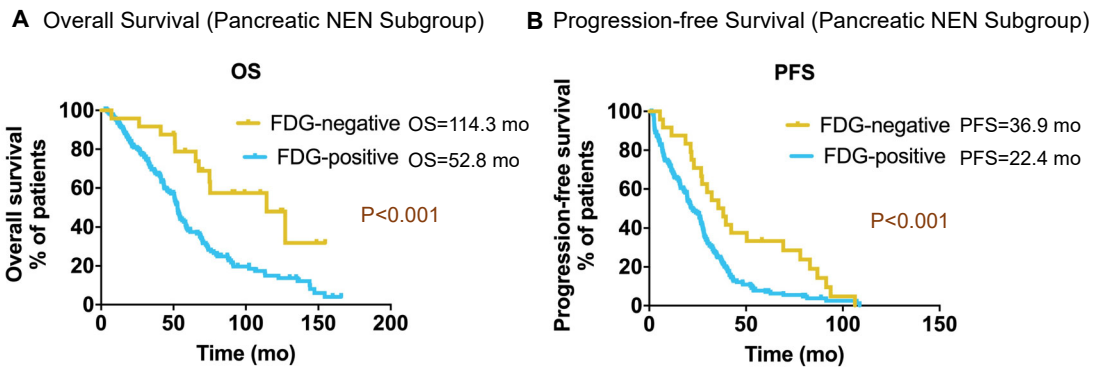

Fig 4. Kaplan-Meier survival of OS (A) and PFS (B) for pancreatic NEN subgroup (n=199) stratified by baseline ^{18}F-FDG status.

Table 1. Demographics of the patients with NENs (n=495)

Characteristic	Number (N)	Percentage (%)
Gender		
Male	299	60.4
Female	196	39.6
Median age — yr	59.0±10.7	
y≤50	111	22.4
50<y≤60	146	29.5
60<y≤70	165	33.3
70<y≤80	73	14.7
Primary tumor site		
CUP	49	9.9
Lung	38	7.7
Midgut	139	28.1
Others	42	8.5
Pancreas	199	40.2
Rectum	20	4.0
Stomach	8	1.6
Ki-67 index grading		
G1 (Ki-67 <3%)	117	23.6
G2 (Ki-67 =3%-20%)	245	49.5
G3 (Ki-67 >20%)	29	5.9
NA	104	21.0

Table 2. Baseline ^{68}Ga-SSTR and ^{18}F-FDG PET imaging of patients with NENs (n=495)

Characteristic	Number (N)	Percentage (%)
PET imaging		
^{68}Ga-SSTR	495	100.0
Level 1 (SUV_{max}=liver)	3	0.6
Level 2 (liver<SUV_{max}≤15)	161	32.5
Level 3 (15<SUV_{max}<20)	106	21.4
Level 4 (SUV_{max}>20)	225	45.5
FDG-PET uptake	495	100.0
Positive	382	77.2
Negative	113	22.8
Uptake of primary tumor		
on FDG PET-CT		
Level 1 (negative/resected)	376	76.0
Level 2 (SUV_{max}≤10)	87	17.6
Level 3 (10<SUV_{max}≤15)	16	3.2
Level 4 (SUV_{max}>15)	16	3.2
on ^{68}Ga-SSTR PET-CT		
Level 1 (negative/resected)	262	52.9
Level 2 (SUV_{max}≤15)	102	20.6
Level 3 (15<SUV_{max}≤20)	37	7.5
Level 4 (SUV_{max}>20)	94	19.0
Tumor burden on FDG-PET		
Liver		
Level 1 (lesion=0)	239	48.3
Level 2 (lesion=1)	49	9.9
Level 3 (2≤lesions≤5)	126	25.5
Level 4 (lesions>5)	77	15.6
NA	4	0.8
Bone		
Level 1 (lesion=0)	409	82.6
Level 2 (lesion=1)	29	5.9
Level 3 (2≤lesions≤5)	36	7.3
Level 4 (lesions>5)	19	3.8
NA	2	0.4
Lymph node		
Level 1 (lesion=0)	362	73.1
Level 2 (lesion=1)	55	11.1
Level 3 (2≤lesions≤5)	58	11.7
Level 4 (lesions>5)	13	2.6
NA	7	1.4
Lungs		
Level 1 (lesion=0)	463	93.5
Level 2 (lesion=1)	22	4.4
Level 3 (2≤lesions≤5)	6	1.2
Level 4 (lesions>5)	4	0.8
Liver tumor burden on ^{68}Ga-SSTR PET		
Level 1 (lesion=0)	76	15.4
Level 2 (lesion=1)	32	6.5
Level 3 (2≤lesions≤5)	153	30.9
Level 4 (lesions>5)	234	47.3
^{68}Ga-SSTR uptake of liver lesions		
Level 1 (no lesion)	77	15.6

Level 1 (SUV_{max}≤15)	117	23.6
Level 1 (15<SUV_{max}≤20)	90	18.2
Level 1 (SUV_{max}>20)	211	42.6

Table 3. Univariate and multivariate analyses of potential factors contributing to OS

Factors	OS (mo)		Univariate analysis (*P*)	Multivariate analysis	
	Median	95%CI		Hazard ratio (95%CI)	*P*
All pts	58.7	52.8-64.6			
Gender					
Male	53.7	47.6-59.8	0.040		
Female	66.1	54.4-77.8			
Age					
y≤50	69.8	61.7-77.8	0.024		
50<y≤60	61.6	51.5-71.7			
60<y≤70	53.0	49.8-56.3			
70<y≤80	49.0	39.6-58.5			
Grading					
G1	78.5	66.2-90.8	<0.001		0.012
G2	55.4	46.9-63.9		1.4 (1.0-2.0)	0.038
G3	33.2	18.8-7.6		2.5 (1.3-4.5)	0.004
NA	54.1	48.3-59.9		1.6 (1.1-2.2)	0.009
FDG-PET uptake					
Positive	53.2	49.4-57.0	<0.001		0.002
Negative	83.1	57.0-109.2		0.5 (0.3-0.8)	
Primary tumor site					
CUP	65.1	47.4-82.7	0.007		0.004
Lung	46.2	34.1-58.3		0.3 (0.1-0.7)	0.004
Midgut	77.8	61.0-94.6		0.7 (0.3-1.6)	0.344
Others	65.7	31.3-100.1		0.3 (0.1-0.7)	0.008
Pancreas	54.4	49.3-59.6		0.4 (0.2-1.0)	0.041
Rectum	55.4	50.3-60.4		0.5 (0.2-1.0)	0.063
Stomach	46.9	33.3-60.5		0.6 (0.2-1.5)	0.239
Tumor burden on FDG-PET					
Liver					
lesion=0	75.6	65.5-85.6	<0.001		0.034
lesion=1	55.4	36.9-73.9		1.7 (0.6-5.2)	0.338
2≤ lesions≤5	47.1	40.5-53.7		1.2 (0.4-3.8)	0.712
lesions>5	43.7	35.4-52.0		2.2 (0.7-6.4)	0.157
NA	54.6	33.7-75.5		2.3 (0.8-7.0)	0.127
Bone					
lesion=0	61.6	54.9-68.3	0.004		
lesion=1	56.0	29.6-82.4			
2≤lesions≤5	41.9	25.1-58.8			
lesions>5	43.4	19.2-67.7			
NA	32.6	-			
Lymph node					
lesion=0	63.8	56.3-71.4	0.006		0.035
lesion=1	51.6	34.6-68. 5		1.4 (0.5-4.1)	0.540
2≤lesions≤5	46.2	37.2-55.3		1.7 (0.6-5.2)	0.344
lesions>5	37.4	10.0-64.7		1.8 (0.6-5.4)	0.293
NA	86.6	23.7-149.6		4.4 (1.3-15.3)	0.018
Grading of PRRT cycles					
2≤cycles≤3	33.27	25.0-41.3	<0.001		<0.001
4≤cycles≤5	51.6	44.5-58.7		7.9 (3.9-15.9)	<0.001
6≤cycles≤7	68.9	61.8-76.1		4.7 (2.6-8.4)	<0.001
8≤cycles≤10	122.5	84.8-160.3		3.0 (1.8-5.0)	<0.001
Cumulative activity (CA) - GBq					
CA≤15	26.0	13.8-38.2	<0.001		0.038

15<CA≤25	52.7	45.4-59.9	1.1 (0.6-2.0)	0.745
25<CA≤35	61.1	54.9-67.3	0.7 (0.4-1.1)	0.084
CA>35	77.8	66.0-89.6	0.8 (0.6-1.2)	0.379

Table 4. Univariate and multivariate analyses of potential factors contributing to PFS

Factors	PFS (mo)		Univariate analysis(P)	Multivariate analysis	
	Median	95%CI		Hazard ratio (95%CI)	*P*
All pts	19.6	17.6-21.7			
Age					
y≤50	25.0	19.4-30.5	0.281		
50<y≤60	18.4	12.8-23.9			
60<y≤70	17.9	15.1-20.7			
70<y≤80	22.4	16.8-28.0			
Grading					
G1	23.0	15.9-30.2	0.003		0.039
G2	18.9	15.2-22.6		1.2(0.9-1.5)	0.150
G3	7.5	0.0-20.1		2.1(1.3-3.4)	0.003
NA	19.8	13.8-25.7		1.1(0.9-1.5)	0.426
FDG-PET uptake					
Positive	18.5	15.9-21.1	0.002		0.007
Negative	24.1	19.9-28.3		0.7(0.5-0.9)	
Primary tumor site					
CUP	11.4	6.5-16.2	0.011		
Lung	10.6	5.0-16.1			
Midgut	22.6	17.2-28.0			
Others	9.1	2.7-15.5			
Pancreas	25.8	21.8-29.8			
Rectum	19.9	11.8-27.9			
Stomach	24.6	18.9-30.4			
Tumor burden on FDG-PET					
Liver					
lesion=0	20.8	17.4-24.1	0.034		
lesion=1	27.8	20.9-34.7			
2≤lesions≤5	16.2	11.5-20.9			
lesions>5	17.9	14.1-21.7			
NA	28.2	0.0-58.7			
Bone					
lesion=0	22.4	19.3-25.5	<0.001		0.001
lesion=1	13.3	1.4-25.1		1.0(0.2-4.1)	0.982
2≤lesions≤5	10.5	8.4-12.5		1.7(0.4-7.4)	0.479
lesions>5	11.5	0.0-24.9		2.2(0.5-9.4)	0.304
NA	12.0	-		1.2(0.3-5.2)	0.848
Lymph node					
lesion=0	21.6	18.6-24.7	<0.001		0.050
lesion=1	17.9	10.9-25.0		1.2(0.5-3.1)	0.587
2≤lesions≤5	15.4	12.3-18.6		1.3(0.5-3.4)	0.552
lesions>5	6.5	4.5-8.5		1.3(0.5-3.3)	0.563
NA	37.2	7.1-67.3		3.5(1.2-10.1)	0.019
Lung					
lesion=0	19.9	17.5-22.3	<0.001		
lesion=1	18.4	16.5-20.3			
2≤lesions≤5	3.7	0.0-21.3			
lesions>5	5.3	1.5-9.2			
Grading of PRRT cycles					
2≤cycles≤3	13.6	8.6-18.5	0.907		
4≤cycles≤5	18.0	15.2-20.8			
6≤cycles≤7	25.0	20.9-29.2			
8≤cycles≤10	26.8	16.7-36.8			

SUPPLEMENTAL MATERIALS AND METHODS

Data Analysis

On ^{18}F-FDG PET imaging, primary tumor uptake was classified into 4 levels: negative/resected, $SUV_{max} \leq 10$, $10 < SUV_{max} \leq 15$, and $SUV_{max} > 15$. Tumor burden (liver, bone and lymph node involvement) assessed by ^{18}F-FDG PET imaging was categorized into 5 levels: no lesion; single lesion; 2≤ lesions ≤5: lesion >5; not assessed. Patients with baseline ^{68}Ga-SSTR imaging were categorized into level 1 (=liver), level 2 (liver$< SUV_{max} \leq 15$), level 3 ($15 < SUV_{max} \leq 20$), level 4 ($SUV_{max} > 20$). On ^{68}Ga-SSTR PET imaging, primary tumor uptake was also classified into 4 levels: negative/resected, $SUV_{max} \leq 15$, $15 < SUV_{max} \leq 20$, and $SUV_{max} > 20$. The classification of liver tumor burden on ^{68}Ga-SSTR PET imaging is the same as ^{18}F-FDG PET imaging.

Supplemental Table 1. Treatment cycles and cumulative administered radioactivity for ^{177}Lu, ^{90}Y and Duo-PRRT with ^{177}Lu and ^{90}Y (N=495)

Variables	N	%	Cumulative radioactivity	
			Mean	SD
Number of PRRT cycles (total)	495	100	25.7	10.8
2	43	8.7	10.0	2.8
3	85	17.2	16.6	4.2
4	102	20.6	21.4	5.0
5	87	17.6	25.8	4.8
6	80	16.2	32.2	6.1
7	56	11.3	35.7	5.7
8	23	4.6	44.4	6.5
9	14	2.8	45.8	7.7
10	5	1.0	49.9	9.4
Number of ^{177}Lu-PRRT cycles (total)	60	12.1	22.2	9.3
2	0	0	0	0
3	16	3.2	19.2	2.7
4	18	4.0	27.3	3.1
5	16	3.2	31.9	0.4
6	7	0.4	41.9	1.1
7	3	1.2	49.7	3.2
8	0	0	0	0
9	0	0	0	0
10	0	0	0	0
Number of ^{90}Y-PRRT cycles (total)	20	4.0	8.7	3.0
2	11	2.2	7.4	2.7
3	5	1.0	10.0	3.4
4	4	0.8	10.8	1.4
5	0	0	0	0
6	0	0	0	0
7	0	0	0	0
8	0	0	0	0
9	0	0	0	0
10	0	0	0	0
Number of Duo-PRRT cycles (total)	415	83.8	27.1	10.5
2	32	6.5	9.9	1.9
3	64	12.9	16.2	4.0
4	80	16.2	20.7	4.0
5	71	14.3	25.6	4.7
6	73	14.7	31.4	5.6
7	53	10.7	35.7	5.7
8	23	4.6	44.4	6.5
9	14	2.8	45.8	7.7
10	5	1.0	49.9	9.4